The Journal of Infectious Diseases

MAJOR ARTICLE

Human Neutralizing Monoclonal Antibody Inhibition of Middle East Respiratory Syndrome Coronavirus Replication in the Common Marmoset

Zhe Chen,[1,a] Linlin Bao,[2,a] Cong Chen,[1,a] Tingting Zou,[3,a] Ying Xue,[1] Fengdi Li,[2] Qi Lv,[2] Songzhi Gu,[2] Xiaopan Gao,[1] Sheng Cui,[1] Jianmin Wang,[1,b] Chuan Qin,[2,b] and Qi Jin[1,4,b]

[1]MOH Key Laboratory of Systems Biology of Pathogens, Institute of Pathogen Biology, Chinese Academy of Medical Sciences & Peking Union Medical College, [2]Institute of Laboratory Animal Sciences, Chinese Academy of Medical Sciences & Peking Union Medical College, Key Laboratory of Human Disease Comparative Medicine, Ministry of Health, Beijing Key Laboratory for Animal Models of Emerging and Remerging Infectious Diseases, [3]College of Life Sciences and Technology, Huazhong Agricultural University, Wuhan, and [4]Collaborative Innovation Center for Diagnosis and Treatment of Infectious Diseases, Hangzhou, China

Middle East respiratory syndrome coronavirus (MERS-CoV) infection in humans is highly lethal, with a fatality rate of 35%. New prophylactic and therapeutic strategies to combat human infections are urgently needed. We isolated a fully human neutralizing antibody, MCA1, from a human survivor. The antibody recognizes the receptor-binding domain of MERS-CoV S glycoprotein and interferes with the interaction between viral S and the human cellular receptor human dipeptidyl peptidase 4 (DPP4). To our knowledge, this study is the first to report a human neutralizing monoclonal antibody that completely inhibits MERS-CoV replication in common marmosets. Monotherapy with MCA1 represents a potential alternative treatment for human infections with MERS-CoV worthy of evaluation in clinical settings.

Key words. human monoclonal antibody; MERS-CoV; common marmoset.

Middle East respiratory syndrome coronavirus (MERS-CoV) was first isolated from the sputum of a 60-year-old Saudi Arabian male patient who eventually died of acute pneumonia [1]. In the past few years, this virus has spread across 27 countries, resulting in >1700 infections and >600 deaths, with a mortality rate of approximately 35% [2–4]. The largest outbreak in South Korea in 2015 caused 186 cases of infection, including 38 deaths [5]. Thus far, all of the reported cases have been linked through travel to or residence in countries in and near the Arabian Peninsula.

Dromedary camels (*Camelus dromedarius*) are regarded as natural reservoirs, in which both neutralizing antibodies and viral RNA have been detected [6–10]. According to nationwide serological tests in Qatar and Saudi Arabia, the proportion of seropositive antibodies was significantly higher in camel-exposed individuals than in the general population [11, 12]. Nucleotide fragments almost identical to the viral genome have also been identified in bats from both Saudi Arabia and Africa, suggesting the likelihood of a bat origin of MERS-CoV [13, 14]. Findings demonstrating that bat coronavirus HKU4 is phylogenetically closely related to MERS-CoV and is capable of using the same cellular receptor also support this possibility [15, 16].

Human dipeptidyl peptidase 4 (DPP4, also called CD26) has been characterized as the cellular receptor for MERS-CoV [17]. Studies have shown that antibodies against receptor-binding domain (RBD) or DPP4 inhibit viral infection in cells [17, 18]. When expressed in mice, the full-length S protein induced the production of neutralizing antibodies against MERS-CoV [19, 20]. Virus-neutralizing activity has also been observed in polyclonal antibodies from mice immunized with truncated RBD protein [21, 22].

MERS-CoV is one of the most threatening pathogens likely to cause major epidemics in the future and has been prioritized in the World Health Organization blueprint for research and development efforts to develop countermeasures [23]. Although ribavirin and interferon exhibited anti–MERS-CoV activity in vitro [24] and alleviated disease symptoms in tested rhesus macaques [25] and some human patients [26], no licensed treatments or vaccines for MERS-CoV infection are currently available. New preventative and therapeutic strategies are urgently needed to counter this global threat. Using viral RBD as bait, scientists have also characterized several monoclonal antibodies (mAbs) with potent neutralizing activities against MERS-CoV from nonimmune human antibody libraries [27, 28]. In particular, a human mAb (m336) directed against the S protein RBD has been described, with potently neutralizing activity in vitro and efficacious in rabbits [29, 30].

In the present study, we isolated a fully human neutralizing antibody against MERS-CoV, MCA1, from the peripheral B cells of a convalescent donor who survived MERS-CoV infection. We report the first evidence that the neutralizing mAb

Received 1 February 2017; editorial decision 25 April 2017; accepted 28 April 2017; published online May 2, 2017.

[a]Z. C., L. B., C. C., and T. Z. contributed equally to this work.

[b]J. W., C. Q., and Q. J. contributed equally to this work.

Correspondence: Q. Jin, MD, MOH Key Laboratory of Systems Biology of Pathogens, Institute of Pathogen Biology, Chinese of Medical Sciences and Peking Union Medical College, 6 Rongjing East Str, BDA, Beijing 100176, P. R. China (zdsys@vip.sina.com).

The Journal of Infectious Diseases® 2017;215:1807–15

DOI: 10.1093/infdis/jix209

MCA1 completely inhibits MERS-CoV replication in nonhuman primates as both a prophylactic and therapeutic. Thus, MCA1 shows promise as a prophylactic or therapeutic for the treatment of human cases of MERS-CoV infection.

MATERIALS AND METHODS

Ethics Statement

The use of human peripheral blood samples was reviewed and approved by the Ethics Committee of the Institute of Pathogen Biology at the Chinese Academy of Medical Sciences and Peking Union Medical College. The patient with severe MERS-COV infection, diagnosed and laboratory confirmed by reverse-transcription polymerase chain reaction, was hospitalized in Huizhou People's Hospital in Guangdong Province, China. Convalescent blood samples were collected after written informed consent was obtained. All animal experiments were approved by the Institutional Animal Care and Use Committee of the Institute of Laboratory Animal Science, Peking Union Medical College, were performed following Chinese national guidelines for the care of laboratory animals, and were approved by the Institutional Animal Care and Use Committee of the Institute of Laboratory Animal Science (protocol no. BLL-16-002). All experiments with live MERS-CoV were performed according to the standard operating procedures of biosafety level 3 facilities, as described elsewhere [31].

Virus Titration

MERS-CoV (EMC/2012 strain), a kind gift from R. A. Fouchier, was subsequently propagated in Vero E6 cells (American Type Culture Collection) in Dulbecco's modified Eagle's medium (DMEM) supplemented with 10% fetal calf serum, penicillin, and streptomycin. The 50% tissue culture infectious doses ($TCID_{50}$) per milliliter was determined for MERS-CoV in Vero E6 cells, as described elsewhere [32].

Selection of MERS-CoV Fragment of Antigen Binding (Fab)

The anti–MERS-CoV phage antibody library was generated as described elsewhere [33]. Briefly, the heavy and light chain genes were amplified from complementary DNA using polymerase chain reaction and were sequentially cloned into the phagemid vector pComb3H for phage library generation. The antibody library was screened through 3 rounds of panning with purified MERS-CoV virions.

Neutralization Assay

MCA1 antibodies were serially diluted in 3-fold steps in DMEM containing 2% fetal calf serum and were inactivated at 56°C for 30 minutes. Subsequently, 50 μL of 100 × $TCID_{50}$ MERS-CoV was combined with each MCA1 dilution and incubated at 37°C for 1 hour. The mixtures (total, 100 μL) were added to Vero E6 cells in 96-well plates and further incubated for 2 hours at 37°C with 5% carbon dioxide. The plates were washed and replaced with DMEM after incubation and were scored for cytopathic effect after 4 days. All experiments were performed under biosafety level 3 conditions.

Common Marmoset Infection Model and Treatment

All experiments involving common marmosets were performed as described elsewhere, with slight modifications, and were approved by the Institutional Animal Care and Use Committee [34, 35]. Briefly, a total of 15 healthy male common marmosets (*Callithrix jacchus*; 2 years old; 230–395 g) were randomly assigned into 5 groups. For measurement of prophylactic efficacy, common marmosets (3 per group) were intraperitoneally inoculated with 5 or 20 mg/kg of purified MCA1 at 24 hours before intratracheal challenge with 5×10^6 $TCID_{50}$ of MERS-CoV in 500 μL of DMEM, under ketamine anesthesia. Three additional common marmosets were infected and used as a model group.

Common marmosets were observed daily for signs of disease and mortality for 3 days. For therapy against MERS disease, 3 other common marmosets were intratracheally infected with 5×10^6 $TCID_{50}$ of MERS-CoV in 500 μL of DMEM and were subsequently passively immunized with 20 mg/kg of purified MCA1 2 or 12 hours later, followed up by daily observations for signs of disease and death for up to 3 days. The animals were observed twice daily for clinical signs and were scored using a described clinical scoring system, described elsewhere, which included the evaluation of the general appearance, skin and fur appearance, discharge (oral, nasal, and/or ocular), respiratory rate, and food consumption [34]. The definition of the clinical score is provided in Supplementary Table 1. Other clinical examinations in the present study included measurements of body temperature (twice daily) and body weight (0, 24, and 72 hours after infection). Necropsies were scheduled at 72 hours after infection or when the clinical score was ≥35, as described elsewhere [25, 34]. Necropsied tissues were collected for histopathology and viral load studies.

Histopathology

Histopathology was performed on marmoset lung tissues. Lung tissue samples from all lobes were resected from formalin-fixed tissue. Lungs were fixed in 10% neutral buffered formaldehyde and embedded in paraffin. Tissue sections (5 μm) were stained with hematoxylin-eosin and analyzed microscopically. Lung pathological findings were recorded by a pathologist blinded to the experimental design, as described elsewhere [36]; findings noted included peribronchiolitis (inflammatory cells, primarily lymphocytes, surrounding a bronchiole), perivasculitis (inflammatory cells, primarily lymphocytes, surrounding a blood vessel), interstitial pneumonitis (increased thickness of alveolar walls associated with inflammatory cells, primarily neutrophils), and alveolitis (inflammatory cells, primarily neutrophils, and macrophages, within alveolar spaces).

Statistical Analysis

The viral titer was independently evaluated for each of the infected common marmosets. All results are presented as means with standard deviations. Statistical analysis was performed using SSPS software, version 10.0. Differences were considered statistically significant at $P < .05$.

Crystallization and Data Collection

Purified MERS-CoV RBD and MCA1 Fab were concentrated to 10 mg/mL in HEPES-buffered saline buffer (10 mmol/L HEPES, pH 7.2, and 150 mmol/L sodium chloride). Viral RBD protein and MCA1 Fab were mixed at 1:1, incubated on ice for 2 hours, and subsequently purified by means of size exclusion chromatography (Superdex 200; GE Healthcare). The complex was collected and concentrated to approximately 10 mg/mL for crystallization screening. Crystallization was successfully realized at 18°C in reservoir solution containing 0.06 mol/L citric acid, 0.04 mol/L bis-tris propane. and 16% (wt/vol) polyethylene glycol 3350. The cryoprotectant was prepared after adding 20% ethylene glycol to the well solution. The diffraction data from the MCA1/RBD crystals were collected at the BL19U beam line at the Shanghai Synchrotron Research Facility. All diffraction images were indexed, integrated, and scaled using HKL2000 software [37].

Structural Determination and Refinement

The structure was determined by molecular replacement methods using the program Phaser in CCP4i (version 7.0.0) [38]. The search model MERS-CoV RBD (Protein Data Bank [PDB] code, 5DO2) for the initial molecular replacement and the structures of variable and constant domains of heavy and light chains are available in the PDB file, showing the highest sequence identities. Iterative refinement with the PHENIX program, version 1.10.1-2155 and model building with the Coot (Crystallographic Object-Oriented Toolkit, Coot 0.8.2) program were performed to complete the structural refinement. Structure validation was performed using the program PROCHECK in CCP4i, and all structural figures were created using PYMOL (version 1.7.4.5). All structural refinement statistics are listed in Table 1. (The crystal structure of MCA1 in complex with MERS-CoV RBD has been deposited in the PDB with accession code 5GMQ.)

RESULTS

Isolation of a Fully Human Neutralizing Antibody Against MERS-CoV

Two Fab phage display libraries (for λ and κ light chains) were established. One Fab antibody that strongly reacted with both antigens, MCA1, was initially isolated and converted into full-length human immunoglobulin G1, with light chain Vκ3 and heavy chain V_H1. The potential neutralizing activity of MCA1 against MERS-CoV was assessed. As shown in Figure 1, MCA1 neutralized MERS-CoV in cells in a dose-dependent manner and showed potent neutralization activity; 0.39 μg/mL completely inhibited live viral replication.

Table 1. Data Collection and Refinement Statistics

	MCA1/MERS-CoV RBD
Data collection	
Space group	P3121
Wavelength, Å	0.979
Unit cell dimensions	
a, *b*, *c*, Å	*a* = *b* = 153.46, *c* = 97.49
α, β, γ, °	90.00, 90.00, 120.00
Resolution, Å	40.33–2.70 (2.80–2.70)[a]
Completeness, %	99.67 (99.35)
Redundancy	6.8 (6.5)
R_{merge}	0.078
I/σ (*I*)	1.68 (2.69)
Refinement	
Resolution, Å	40.33–2.70 (2.80–2.70)
Unique reflections	36 296 (3599)
Completeness, %	99.35 (99.67)
R_{work}/R_{free}	0.2392/0.2846
Atoms, No.	
Protein	4876
Ligands	55
Water	16
B factor, Å^2	
Protein	49.2
Ligands	60.0
Solvent	37.2
Root-mean-square deviations	
Bond length, Å	0.011
Bond angle	1.4°
Ramachandran plot	
Most favored, %	92.22
Generally allowed, %	6.83
Disallowed, %	0.98

[a]Values in parentheses are for the highest-resolution data shell. $R_{merge} = \Sigma_{hkl} | I_{avg} - I_i | / \Sigma_{hkl} I_i$.

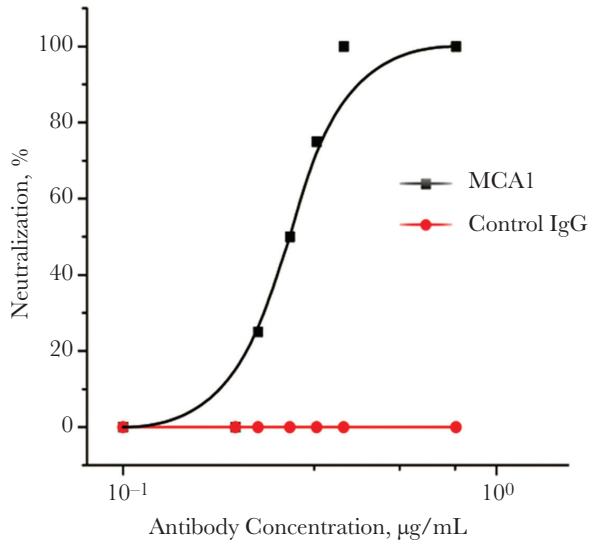

Figure 1. MCA1 neutralized Middle East respiratory syndrome coronavirus (MERS-CoV) in vitro. The neutralizing activities of MCA1 against MERS-CoV were examined using Vero E6 cells. An irrelevant human immunoglobulin G (IgG) was used as a control.

Prophylactic Efficacy of MCA1 in the Common Marmoset

To explore the prophylactic efficacy of MCA1, common marmosets were intravenously inoculated with the antibody at doses of 5 mg/kg (designated G1) and 20 mg/kg (G2) and then challenged with MERS-CoV 24 hours later. A control group was simultaneously infected and set up as a model (M) group. The clinical signs, temperature changes, and body weight changes in the marmosets were monitored daily. Severe disease developed in model animals, with increased respiratory rates, reduced movement, and loss of appetite as soon as 12 hours after viral infection.

As shown in Figure 2A, the mean clinical score of the M group animals was 2 at 12 hours after infection, reaching 11.7 at 72 hours after infection. The mean clinical scores for the MCA1-treated groups were less than those for the M group, particularly for the G2 group. By the end of the monitoring period, the mean clinical score for G2 common marmosets was nearly 50% less than that for the M group. The mean body temperature for the common marmosets in M and G1 peaked to >40°C at 12 hours after infection (Figure 2B). In contrast, the mean temperature for the G2 group gradually changed and remained at nearly normal body temperature until the end of the experiment (Figure 2B). As a result of viral infection, all the common marmosets showed some body weight loss after infection. At 3 days after infection, those in the M group showed >10% body weight loss, compared with losses of <7% and <2%, respectively, in the G1 and G2 groups (Figure 2C). Taken together, these results demonstrated that MCA1, when prophylactically immunized, substantially improved the clinical outcomes of common marmosets infected with MERS-CoV.

Therapeutic Treatment of MERS-CoV Infection With MCA1 in Common Marmosets

To clarify the clinically relevant effect of antiviral therapy against MERS-CoV infection, the common marmosets were initially intratracheally infected with 5×10^6 $TCID_{50}$ of MERS-CoV, followed by intravenous inoculation with MCA1 at 2 (G3) or 12 (G4) hours, at 20 mg/kg. The efficacy of the treatment was determined. At 72 hours after infection, the mean clinical score for the G3 group was 2.7, compared with 6.3 for the G4 group, and both lower scores than for the M group (Figure 3A).

Mean body temperature changes are shown in Figure 3B. In the G3 group, mean body temperature did not change much during the entire experiment, whereas in the G4 group, the mean body temperature peaked at 12 hours after infection, at >41°C. Similarly, all common marmosets showed body weight losses in response to viral infection. However, those in the G3 group received MCA1 treatment earlier and lost <4% body weight compared with approximately 10% for the common marmosets in the M and G4 groups (Figure 3C). These results demonstrated that MCA1, even when inoculated after infection, improved the circumstances of common marmosets with MERS-CoV infection.

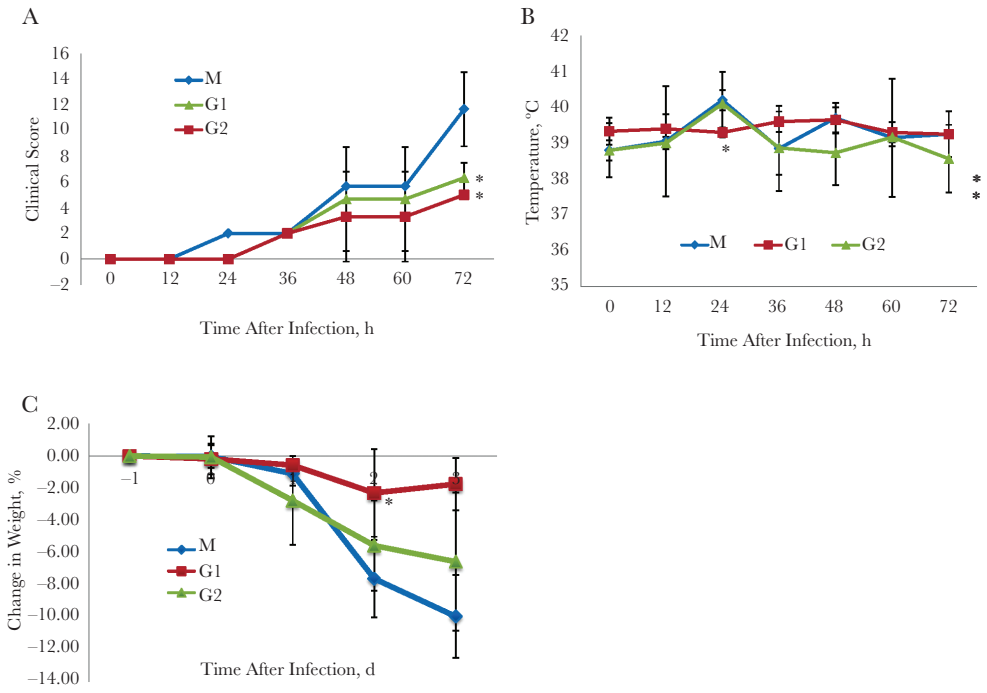

Figure 2. Prophylactic efficacy of MCA1 in common marmosets, which were intravenously inoculated with the antibody at doses of 5 mg/kg (designated G1) and 20 mg/kg (G2) and then challenged with Middle East respiratory syndrome coronavirus (MERS-CoV) 24 hours later. A control group was simultaneously infected and set up as a model (M) group. All groups were monitored twice daily for 3 days. *A,* Clinical scores (n = 3 per group). *B,* Temperature changes (n = 3 per group). *C,* Mean body weight changes (n = 3 per group). Results are presented as means with standard deviations. *$P < .05$ (*t* test).

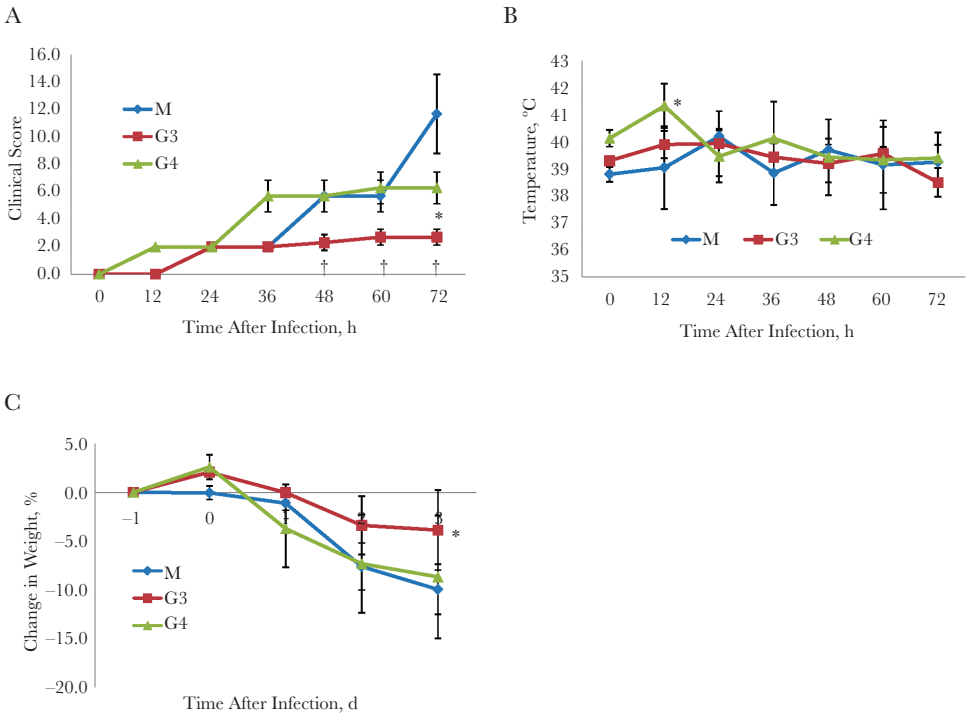

Figure 3. Therapeutic treatment using MCA1 in common marmosets, which were initially intratracheally infected with Middle East respiratory syndrome coronavirus (MERS-CoV), followed by intravenous inoculation with MCA1 at 2 (G3) or 12 (G4) hours, at 20 mg/kg. A control group was simultaneously infected and set up as a model (M) group. *A,* Clinical scores (n = 3 per group). *B,* Temperature changes (n = 3 per group). *C,* Mean body weight changes (n = 3 per group). Results are presented as means with standard deviations. $^{*}P < .05$; $^{\dagger}P < .01$ (*t* test).

Reduction of Lung Disease and Viral Replication by MCA1 Treatment

Histopathology detection demonstrated that the model group showed severe, multifocal to coalescing acute bronchointerstitial pneumonia (Figure 4A). Pulmonary alveoli were infiltrated by a significant amount of inflammatory cells, predominantly consisting of macrophages, neutrophils, and lymphocytes. The alveolar interstitium was thickened with edema, fibrin, and hemorrhage. In contrast, all common marmosets that received MCA1 treatment, both before and after exposure, showed mild to moderate bronchointerstitial pneumonia, with small amounts of inflammatory cell infiltrates, edema, and hemorrhage (Figure 4A). Expectedly, the mean viral titer was high in the common marmosets, with the highest viral titer of >5.5 $\log_{10}$ $TCID_{50}$ per gram detected in the lobes of the lungs; the viral titer was also up to 2 $\log_{10}$ $TCID_{50}$ in the trachea (Figure 4B). In contrast, no viral titers were detected in MCA1-treated animals. These results demonstrated that MCA1 substantially inhibited MERS-CoV replication in vivo.

Structural Basis for Neutralization by MCA1

To further elucidate the neutralization mechanisms and the epitopes for vaccine development, crystallization of the MCA1/MERS-CoV RBD complex was successfully obtained and solved at a resolution of 2.7 Å (Supplementary Table 3). After several rounds of refinement and manual model building, the working *R* factor and *R*-free value of the final atomic model were 23.92% and 28.46%, respectively. One MCA1/MERS-CoV RBD complex was obtained in the crystallographic asymmetric unit at a binding ratio of 1:1. In this model, 1 ethylene glycol molecule existed between the heavy and light chains. Moreover, 4 N-glycans (2 N-acetyl-D-glucosamines and 2 mannoses) linked together and subsequently attached to residue N487 of the RBD (Figure 5A).

The MCA1 antibody formed direct contacts with the receptor-binding site (RBS) subdomain on the RBD, with all 6 complementarity-determining regions (CDRs) surrounding this site (Figure 5B). Both the heavy and light chains of MCA1 primarily contributed to the paratope via the CDRs, with a buried surface area of approximately 835.3 $Å^2$ in the viral ligand for the heavy chain and 126.7 $Å^2$ for the light chain. Obviously, the heavy-chain variable domain contributed to a majority of the binding surface. As shown in Figure 5C, 3 CDRs of the heavy chain formed a hydrophobic cavity and encompassed the epitope on the RBS. The interaction residues of the MCA1 Fab included F26, S27, and S28 in H1, G98, D99, T100, and R103 in H3, and G91 in L3. Two salt bridges were formed by residue R103. The epitope on the RBS consisted of D539, Y540, R542, and Q544 in the β7 strand, E536 and W535 in a long loop, and D510 in a short loop.

We further superimposed the MCA1/MERS-CoV RBD with the previously reported structure of the human DPP4/MERS-CoV RBD complex (PDB code, 4L72). As shown in Figure 5D,

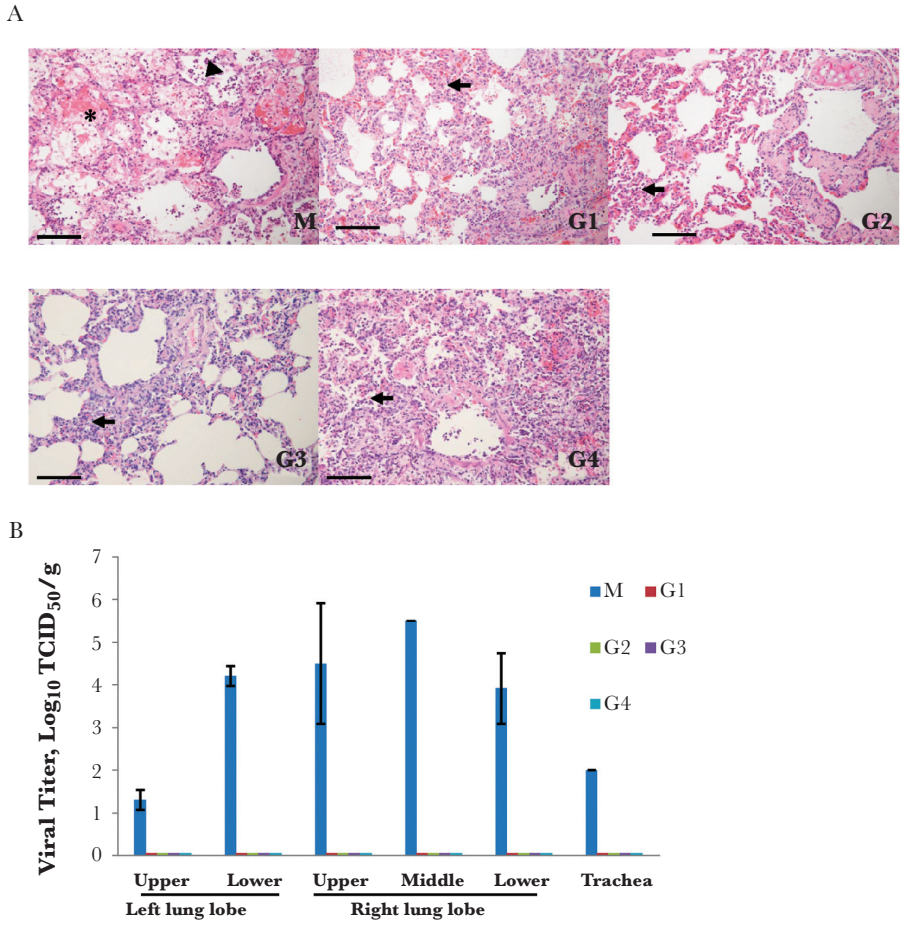

Figure 4. Histopathology and viral titer detection. The common marmosets, were intravenously inoculated with MCA1 at doses of 5 mg/kg (G1) and 20 mg/kg (G2) and then challenged with Middle East respiratory syndrome coronavirus (MERS-CoV) 24 hours later, or were initially intratracheally infected with MERS-CoV, followed by intravenous inoculation with MCA1 at 2 (G3) or 12 (G4) hours, at 20 mg/kg. A control group was simultaneously infected and set up as a model (M) group. *A,* Histopathological appearance of pulmonary tissue from MERS-CoV–infected marmosets. Lungs of marmosets in the model group (M) showed acute bronchointerstitial pneumonia; the pulmonary alveoli were infiltrated by a large amount of inflammatory cells (*arrowhead*), with fibrin exudation (*asterisk*). The alveolar interstitium were thickened and pulmonary alveoli were filtrated by inflammatory cells (*arrows*) in the G1, G2, G3, and G4 groups. Scale bar, 100 μm. *B,* Viral titers from lung and trachea were determined 3 days after infection.

human DPP4 interacted with the viral RBD at the β-propeller domain. The MCA1 Fab epitope surface generated steric clashes at the upside of the β7 strand on the RBS, and the binding interface of the MCA1 Fab largely overlapped with the DPP4-binding site.

DISCUSSION

In recent years, the continuous emergence of zoonotic viruses has posed serious global threats to public health, such as severe acute respiratory syndrome coronavirus [39], H5N1 [40], MERS-CoV [1], H7N9 [33], Ebola [41], and Zika [24]. Unfortunately, the development of a vaccine or an antiviral agent is time consuming and lagging. With the promotion of antibody production technologies, human antibodies will gain more uses, as they have been demonstrated as more secure and effective. Previously, our group isolated neutralizing antibodies from patients who recovered from H7N9 infection [42, 43]. Here, we report the generation of a fully human neutralizing antibody, MCA1, which binds to the MERS-CoV RBD. We provided the first evidence that MCA1 completely inhibits MERS-CoV replication in nonhuman primates, and results have shown that both the severity and the area of bronchointerstitial pneumonia were improved to certain degrees.

With a few exceptions, in vivo data associated with the use of convalescent plasma or mAbs for the treatment of MERS are lacking [44]. Previous studies have primarily focused on mouse models transduced with an adenovirus vector expressing the human DPP4 receptor to evaluate the effect of antibodies against MERS infection. However, nonhuman primate models, which faithfully mimic human disease to a maximum extent, will provide a better understanding of the pathogenesis of MERS-CoV in humans and will be effective models for evaluating the efficacy of potential treatment strategies [45].

The antibody 3B11 was isolated from a nonimmune human phage antibody library [27]. To our knowledge, this antibody has been the only MERS-CoV–neutralizing antibody examined in rhesus monkeys, resulting in mild and self-limiting diseases

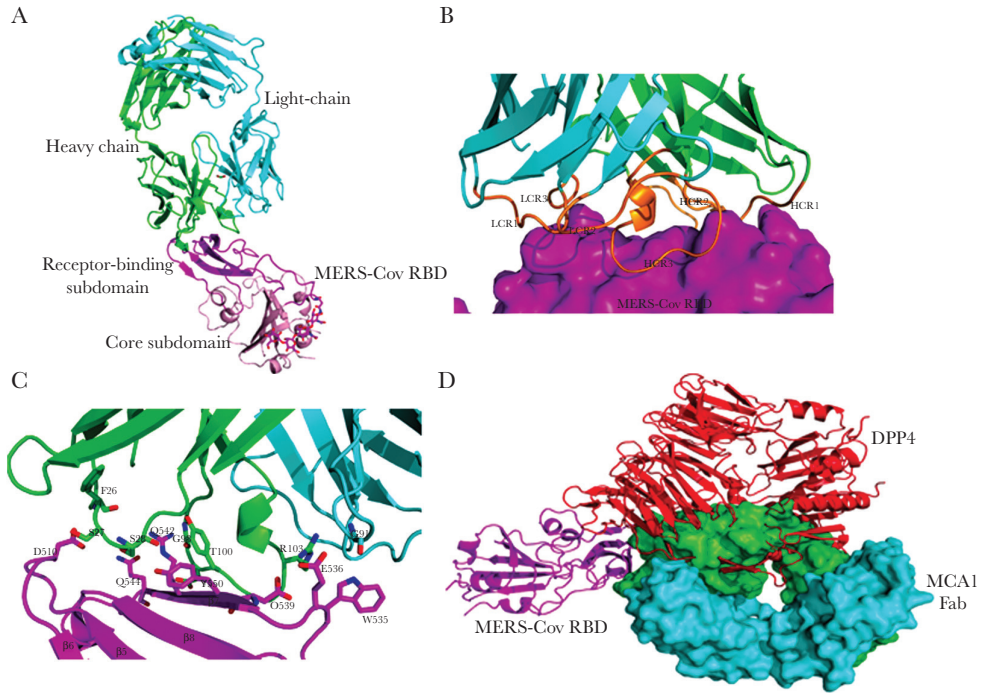

Figure 5. Crystal structures of MCA1 fragment of antigen binding (Fab) in complex with Middle East respiratory syndrome coronavirus (MERS-CoV) receptor-binding domain (RBD). *A,* Crystal structure of MCA1/MERS-CoV RBD complex in graphic representation. The receptor-binding site (RBS) and core subdomain of MERS-CoV RBD are colored light pink and magenta, respectively; the heavy chain is green, and the light chain cyan. The ethylene glycol between the heavy and light chains and the N-linked glycans in the RBD are represented as magentas sticks. *B,* Closer view of the interaction between MCA1 Fab and the RBS. The RBS is depicted in surface representation. Three complementarity-determining regions (CDRs) of the heavy and light chains are colored orange. *C,* Detailed interactions between MCA1 and the RBS. Key residues are shown as sticks. *D,* Superimposed structures of MERS-CoV RBD binding to MCA1 and dipeptidyl peptidase (DPP4). The heavy and light chains of MCA1 are depicted in surface representation, and DPP4 is shown in red.

[46]. Treatment with 3B11 reduced lung pathology in infected rhesus monkeys; however, because viral RNA was undetectable in both model and neutralizing antibody–treated animals, the precise in vivo inhibitory effect of this antibody remains hard to determine. As the only neutralizing antibody from a MERS-CoV survivor, LCA60 was capable of higher neutralizing activity (showing 10-fold more potency than 3B11) [47]. However, the anti-MERS efficacy for LCA60 in primates has not yet been reported. Another nonhuman primate model with the common marmoset has been developed, in which marmosets are intratracheally infected with MERS-CoV. This model supports viral growth and shows evidence of histological lesions, progressive severe pneumonia, and high viral titers in the lungs and trachea, mimicking severe MERS disease in humans, which will ensure a better preclinical analysis of treatments before proceeding to clinical trials in humans [34].

In the present study, we also took advantage of the common marmoset to assess the prophylactic and therapeutic efficacies of MCA1. All M groups developed serious MERS disease and suffered from fever and noticeable body weight losses. Treatment with MCA1, both before and after exposure to viral infection, improved the clinical and pathological features in the infected marmosets. No viral titer was detected in MCA1-treated animals at 3 days after infection in both prophylactic and therapeutic experiments. In contrast, the mean viral titer in the lobes of the lungs reached peak values at 3 days after infection, which was >5.5 $\log_{10}$ $TCID_{50}$ per gram in the M group. The results of prophylactic experiments showed that MCA1 will be beneficial to the prevention of a MERS outbreak, serving as a prophylactic for high-risk individuals exposed to MERS-CoV. Because the 5-mg/kg treatment dose was effective, large inoculum volumes are not required. Viral replication and titer are important during the course of disease development [48]. In a previous study, viral replication was not completely inhibited [44]. However, the results of the present study showed that viral replication could be completely inhibited using MCA1 in common marmosets.

Preliminary research data showed that marmosets infected with MERS-CoV exhibited obvious focal pneumonia after 24 hours. In the present study, all model common marmosets also showed severe pathological changes in the lungs at 3 days after infection. In MCA1-treated animals, both the severity and the area of bronchointerstitial pneumonia were improved to certain degrees. Histopathology detection also showed that the effects in the high-dose prophylaxis group (20 mg/kg) were better than those in the low-dose prophylaxis group (5 mg/kg), and the effects in the therapeutic group at 2 hours after infection were better than those in the therapeutic group after12 hours. Thus, we proposed that the histopathological changes in the

lungs were associated with the doses and course of MCA1. In conclusion, MCA1 suppressed MERS-CoV replication and reduced inflammatory responses to certain degrees. These findings could be applied in future clinical studies.

Previous studies have shown that neutralizing mAbs primarily target the RBD of the MERS-CoV spike glycoprotein. The DPP4-binding site on the viral RBD can be separated into 2 major binding patches [49]. Structural analysis of the MCA1/MERS-CoV RBD interactions revealed a binding interface almost completely encompassing both patches on the RBD. Among these residues, W535 primarily bound to G91 of the light chain, and other residues involved in interactions with the heavy chain of MCA1. Moreover, residues Y540, R542, and Q544 on the RBD formed the hydrophobic cavity and interacted with the surrounding MCA1 residues G98, D99, T100, and S28 of the heavy chain. It is plausible that MCA1 forms hydrogen bonds with the epitopes on the RBD and occupies the binding sites for DPP4, interfering with viral recognition of the human cellular receptor.

In summary, MCA1 completely inhibits MERS-CoV replication in nonhuman primates in both prophylactic and therapeutic treatments. It should be considered a promising candidate in clinical trials, reflecting its safety, potent neutralizing activity and excellent performance in vivo. Thus, we propose that MCA1 plays an important role in preventing MERS-COV infection and warrants further development as a medical countermeasure against MERS-COV infection.

Supplementary Data

Supplementary materials are available at *The Journal of Infectious Diseases* online. Consisting of data provided by the authors to benefit the reader, the posted materials are not copyedited and are the sole responsibility of the authors, so questions or comments should be addressed to the corresponding author.

Notes

Acknowledgments. We thank the Scripps Institute for providing the pComb3H and PIGG vectors. We thank the staff at the Shanghai Synchrotron Radiation Facility (beam line BL19U1 and BL17U) for help with the data collection.

Financial support. This study was supported by the CAMS Innovation Fund for Medical Sciences (grant 2016-I2M-1–014), the Chinese National Major S & T Project (grant 2013ZX10004-101), the National Key Plan for Scientific Research and Development of China (grant 2016YFD0500300), and the National Science Foundation of China (grants 31500757 and 31400787) from the National Science Foundation.

Potential conflicts of interest. All authors: No reported conflicts of interest. All authors have submitted the ICMJE Form for Disclosure of Potential Conflicts of Interest. Conflicts that the editors consider relevant to the content of the manuscript have been disclosed.

References

1. Zaki AM, van Boheemen S, Bestebroer TM, Osterhaus AD, Fouchier RA. Isolation of a novel coronavirus from a man with pneumonia in Saudi Arabia. N Engl J Med **2012**; 367:1814–20.
2. Zumla A, Hui DS, Perlman S. Middle East respiratory syndrome. Lancet **2015**; 386:995–1007.
3. Assiri A, McGeer A, Perl TM, et al; KSA MERS-CoV Investigation Team. Hospital outbreak of Middle East respiratory syndrome coronavirus. N Engl J Med **2013**; 369:407–16.
4. Modjarrad K, Moorthy VS, Ben Embarek P, Van Kerkhove M, Kim J, Kieny MP. A roadmap for MERS-CoV research and product development: report from a World Health Organization consultation. Nat Med **2016**; 22:701–5.
5. Kim SW, Yang TU, Jeong Y, et al. Middle East respiratory syndrome coronavirus outbreak in the Republic of Korea, 2015. Osong Public Health Res Perspect **2015**; 6:269–78.
6. Reusken CB, Haagmans BL, Müller MA, et al. Middle East respiratory syndrome coronavirus neutralising serum antibodies in dromedary camels: a comparative serological study. Lancet Infect Dis **2013**; 13:859–66.
7. Muller MA, Corman VM, Jores J, et al. MERS coronavirus neutralizing antibodies in camels, Eastern Africa, 1983–1997. Emerg Infect Dis **2014**; 20:2093–5.
8. Haagmans BL, Al Dhahiry SH, Reusken CB, et al. Middle East respiratory syndrome coronavirus in dromedary camels: an outbreak investigation. Lancet Infect Dis **2014**; 14:140–5.
9. Memish ZA, Cotten M, Meyer B, et al. Human infection with MERS coronavirus after exposure to infected camels, Saudi Arabia, 2013. Emerg Infect Dis **2014**; 20:1012–5.
10. Azhar EI, El-Kafrawy SA, Farraj SA, et al. Evidence for camel-to-human transmission of MERS coronavirus. N Engl J Med **2014**; 370:2499–505.
11. Müller MA, Meyer B, Corman VM, et al. Presence of Middle East respiratory syndrome coronavirus antibodies in Saudi Arabia: a nationwide, cross-sectional, serological study. Lancet Infect Dis **2015**; 15:629.
12. Reusken CB, Farag EA, Haagmans BL, et al. Occupational exposure to dromedaries and risk for MERS-CoV infection, Qatar, 2013–2014. Emerg Infect Dis **2015**; 21:1422–5.
13. Memish ZA, Mishra N, Olival KJ, et al. Middle East respiratory syndrome coronavirus in bats, Saudi Arabia. Emerg Infect Dis **2013**; 19:1819–23.
14. Ithete NL, Stoffberg S, Corman VM, et al. Close relative of human Middle East respiratory syndrome coronavirus in bat, South Africa. Emerg Infect Dis **2013**; 19:1697–9.
15. Woo PC, Lau SK, Li KS, Tsang AK, Yuen KY. Genetic relatedness of the novel human group C betacoronavirus to *Tylonycteris* bat coronavirus HKU4 and *Pipistrellus* bat coronavirus HKU5. Emerg Microbes Infect **2012**; 1:e35.
16. Wang Q, Qi J, Yuan Y, et al. Bat origins of MERS-CoV supported by bat coronavirus HKU4 usage of human receptor CD26. Cell Host Microbe **2014**; 16:328–37.
17. Raj VS, Mou H, Smits SL, et al. Dipeptidyl peptidase 4 is a functional receptor for the emerging human coronavirus-EMC. Nature **2013**; 495:251–4.
18. Ohnuma K, Haagmans BL, Hatano R, et al. Inhibition of Middle East respiratory syndrome coronavirus infection by anti-CD26 monoclonal antibody. J Virol **2013**; 87:13892–9.
19. Song F, Fux R, Provacia LB, et al. Middle East respiratory syndrome coronavirus spike protein delivered by modified vaccinia virus Ankara efficiently induces virus-neutralizing antibodies. J Virol **2013**; 87:11950–4.
20. Volz A, Kupke A, Song F, et al. Protective efficacy of recombinant modified Vaccinia virus Ankara delivering Middle East respiratory syndrome coronavirus spike glycoprotein. J Virol **2015**; 89:8651–6.
21. Mou H, Raj VS, van Kuppeveld FJ, Rottier PJ, Haagmans BL, Bosch BJ. The receptor binding domain of the new Middle East respiratory syndrome coronavirus maps to a 231-residue region in the spike protein that efficiently elicits neutralizing antibodies. J Virol **2013**; 87:9379–83.
22. Du L, Zhao G, Kou Z, et al. Identification of a receptor-binding domain in the S protein of the novel human coronavirus Middle East respiratory syndrome coronavirus as an essential target for vaccine development. J Virol **2013**; 87:9939–42.
23. World Health Organization. WHO publishes list of top emerging diseases likely to cause major epidemics. 10 December 2015. http://www.who.int/medicines/ebola-treatment/WHO-list-of-top-emerging-diseases/en/. Accessed .
24. Lanciotti RS, Kosoy OL, Laven JJ, et al. Genetic and serologic properties of Zika virus associated with an epidemic, Yap State, Micronesia, 2007. Emerg Infect Dis **2008**; 14:1232–9.
25. Cheng Y, Wong R, Soo YO, et al. Use of convalescent plasma therapy in SARS patients in Hong Kong. Eur J Clin Microbiol Infect Dis **2005**; 24:44–6.
26. Al-Tawfiq JA, Momattin H, Dib J, Memish ZA. Ribavirin and interferon therapy in patients infected with the Middle East respiratory syndrome coronavirus: an observational study. Int J Infect Dis **2014**; 20:42–6.
27. Tang XC, Agnihothram SS, Jiao Y, et al. Identification of human neutralizing antibodies against MERS-CoV and their role in virus adaptive evolution. Proc Natl Acad Sci U S A **2014**; 111:2018–26.
28. Jiang L, Wang N, Zuo T, et al. Potent neutralization of MERS-CoV by human neutralizing monoclonal antibodies to the viral spike glycoprotein. Sci Transl Med **2014**; 6:234ra59.
29. Houser KV, Gretebeck L, Ying T, et al. Prophylaxis with a Middle East respiratory syndrome coronavirus (MERS-CoV)-specific human monoclonal antibody protects rabbits from MERS-CoV infection. J Infect Dis **2016**; 213:1557–61.

30. Ying T, Du L, Ju TW, et al. Exceptionally potent neutralization of Middle East respiratory syndrome coronavirus by human monoclonal antibodies. J Virol **2014**; 88:7796–805.
31. Du L, Jiang S. Middle East respiratory syndrome: current status and future prospects for vaccine development. Expert Opin Biol Ther **2015**; 15:1647–51.
32. Zhou J, Chu H, Li C, et al. Active replication of Middle East respiratory syndrome coronavirus and aberrant induction of inflammatory cytokines and chemokines in human macrophages: implications for pathogenesis. J Infect Dis **2014**; 209:1331–42.
33. Gao R, Cao B, Hu Y, et al. Human infection with a novel avian-origin influenza A (H7N9) virus. N Engl J Med **2013**; 368:1888–97.
34. Falzarano D, de Wit E, Feldmann F, et al. Infection with MERS-CoV causes lethal pneumonia in the common marmoset. PLoS Pathog **2014**; 10:e1004250.
35. Yao Y, Bao L, Deng W, et al. An animal model of MERS produced by infection of rhesus macaques with MERS coronavirus. J Infect Dis **2014**; 209:236–42.
36. Chen HD, Fraire AE, Joris I, Welsh RM, Selin LK. Specific history of heterologous virus infections determines anti-viral immunity and immunopathology in the lung. Am J Pathol **2003**; 163:1341–55.
37. Otwinowski Z, Minor W. Processing of X-ray diffraction data collected in oscillation mode. Methods Enzymol **1997**; 276:307–26.
38. McCoy AJ. Solving structures of protein complexes by molecular replacement with Phaser. Acta Crystallogr D Biol Crystallogr **2007**; 63:32–41.
39. Rota PA, Oberste MS, Monroe SS, et al. Characterization of a novel coronavirus associated with severe acute respiratory syndrome. Science **2003**; 300:1394–9.
40. Ungchusak K, Auewarakul P, Dowell SF, et al. Probable person-to-person transmission of avian influenza A (H5N1). N Engl J Med **2005**; 352:333–40.
41. Baize S, Pannetier D, Oestereich L, et al. Emergence of Zaire Ebola virus disease in Guinea. N Engl J Med **2014**; 371:1418–25.
42. Chen Z, Wang J, Bao L, et al. Human monoclonal antibodies targeting the haemagglutinin glycoprotein can neutralize H7N9 influenza virus. Nat Commun **2015**; 6:6714.
43. Wang J, Chen Z, Bao L, et al. Characterization of two human monoclonal antibodies neutralizing influenza A H7N9 viruses. J Virol **2015**; 89:9115–8.
44. De WE, Van DN, Falzarano D, et al. SARS and MERS: recent insights into emerging coronaviruses. Nat Rev Microbiol **2016**; 14:523–34
45. de Wit E, Rasmussen AL, Falzarano D, et al. Middle East respiratory syndrome coronavirus (MERS-CoV) causes transient lower respiratory tract infection in rhesus macaques. Proc Natl Acad Sci U S A **2013**; 110:16598–603.
46. Johnson RF, Bagci U, Keith L, et al. 3B11-N, a monoclonal antibody against MERS-CoV, reduces lung pathology in rhesus monkeys following intratracheal inoculation of MERS-CoV Jordan-n3/2012. Virology **2016**; 490:49–58.
47. Corti D, Zhao J, Pedotti M, et al. Prophylactic and postexposure efficacy of a potent human monoclonal antibody against MERS coronavirus. Proc Natl Acad Sci U S A **2015**; 112:10473–8.
48. Tao X, Garron T, Agrawal AS, et al. Characterization and demonstration of value of a lethal mouse model of Middle East respiratory syndrome coronavirus infection and disease. J Virol **2015**; 90:57–67.
49. Wang N, Shi X, Jiang L, et al. Structure of MERS-CoV spike receptor-binding domain complexed with human receptor DPP4. Cell Res **2013**; 23:986–93.